



# Mapping of pathological change in chronic fatigue syndrome using the ratio of T1- and T2-weighted MRI scans

Kiran Thapaliya<sup>a,b,\*</sup>, Sonya Marshall-Gradisnik<sup>a</sup>, Don Staines<sup>a</sup>, Leighton Barnden<sup>a</sup>

<sup>a</sup> National Centre for Neuroimmunology and Emerging Diseases, Menzies Health Institute Queensland, Griffith University, Australia

<sup>b</sup> Centre for Advanced Imaging, The University of Queensland, Australia

## ARTICLE INFO

### Keywords:

Myalgic encephalomyelitis/Chronic fatigue syndrome  
T1weighted  
T2weighted  
T1w/T2w ratio  
Myelin  
Iron  
White matter  
Basal ganglia  
Tissue microstructure

## ABSTRACT

Myalgic Encephalomyelitis or Chronic Fatigue Syndrome (ME/CFS) subjects suffer from a variety of cognitive complaints indicating that the central nervous system plays a role in its pathophysiology. Recently, the ratio T1w/T2w has been used to study changes in tissue myelin and/or iron levels in neurodegenerative diseases such as multiple sclerosis and schizophrenia. In this study, we applied the T1w/T2w method to detect changes in tissue microstructure in ME/CFS patients relative to healthy controls. We mapped the T1w/T2w signal intensity values in the whole brain for forty-five ME/CFS patients who met Fukuda criteria and twenty-seven healthy controls and applied both region- and voxel-based quantification. We also performed interaction-with-group regressions with clinical measures to test for T1w/T2w relationships that are abnormal in ME/CFS at the population level. Region-based analysis showed significantly elevated T1w/T2w values (increased myelin and/or iron) in ME/CFS in both white matter (WM) and subcortical grey matter. The voxel-based group comparison with sub-millimetre resolution voxels detected very significant clusters with increased T1w/T2w in ME/CFS, mostly in subcortical grey matter, but also in brainstem and projection WM tracts. No areas with decreased T1w/T2w were found in either analysis. ME/CFS T1w/T2w regressions with heart-rate variability, cognitive performance, respiration rate and physical well-being were abnormal in both gray and white matter foci. Our study demonstrates that the T1w/T2w approach is very sensitive and shows increases in myelin and/or iron in WM and basal ganglia in ME/CFS.

## 1. Introduction

Myalgic Encephalomyelitis or Chronic Fatigue Syndrome (ME/CFS), is a complex illness characterised by profound fatigue of > 6 months duration, autonomic, cognitive and motor dysfunction, and unrefreshing sleep (Fukuda, 1994). The severity of ME/CFS has been classified according to the Fukuda criteria (Fukuda, 1994). Patients who suffer from ME/CFS report a variety of physical complaints (primarily post-exertional malaise) as well as cognitive symptoms (deficits in memory, attention, reaction time, information processing speed and free memory recall) (Cockshell and Mathias, 2010) and ME/CFS is more prevalent in females (Faro et al., 2016). The involvement of the central nervous system (CNS) in ME/CFS cognitive symptoms has been investigated with the non-invasive techniques of PET/SPECT and magnetic resonance imaging (MRI) (Schwartz et al., 1994; Zeineh et al., 2014).

Structurally and functionally, brain MRI scans have been used to provide complementary information on the underlying ME/CFS

pathomechanism (Zeineh et al., 2014; Finkelmeyer et al., 2018; de Lange et al., 2005; Barnden et al., 2018; Puri et al., 2012). Buchwald et al. (Buchwald et al., 1992) reported a higher percentage (78%) of abnormal brain scans in ME/CFS patients in comparison to healthy controls (21%). Other studies showed increases in prefrontal cortical volume and cortical thickness (de Lange et al., 2005), decreases in global grey and white matter volumes (Okada et al., 2004), and regional volume decreases in the frontal cortex, limbic areas, basal ganglia, thalami and brain stem (Puri et al., 2012; Barnden et al., 2015) in ME/CFS, although some results were not reproduced elsewhere. Blood-oxygen-level-dependent (BOLD) functional MRI (fMRI) studies have shown reduced ME/CFS connectivity within the brain stem (Barnden et al., 2019) and decreased functional connectivity in primary neurocognitive networks (Boissoneault et al., 2016). A diffusion study showed atrophy in bilateral white matter and higher fractional anisotropy (FA) in the right arcuate fasciculus (Zeineh et al., 2014). Increased white matter hyperintensities were also reported using T1 and T2 weighted MRI data in ME/CFS patients (Barnden et al., 2018;

\* Corresponding author.

E-mail address: [k.thapaliya@griffith.edu.au](mailto:k.thapaliya@griffith.edu.au) (K. Thapaliya).

<https://doi.org/10.1016/j.nicl.2020.102366>

Received 14 June 2020; Received in revised form 28 July 2020; Accepted 29 July 2020

Available online 31 July 2020

2213-1582/ © 2020 Published by Elsevier Inc. This is an open access article under the CC BY-NC-ND license (<http://creativecommons.org/licenses/by-nc-nd/4.0/>).

Natelson et al., 1993). However, increased signal intensity in T1 and T2 weighted images are inconsistent across studies (Cope and David, 1996).

Recently, T1weighted (T1w) and T2weighted (T2w) images were combined to assess tissue microstructure via T1w/T2w maps (Ganzetti et al., 2014). The T1w/T2w method is popular compared to fMRI and DTI in research and clinical settings due to fast scan times, relatively simple image post processing, reliability and repeatability in measurement (Uddin et al., 2018). T1w images have higher white matter (WM) signal intensity relative to grey matter (GM) and cerebrospinal fluid (CSF) whereas T2w images have lower WM signal intensity relative to GM and CSF. Therefore, T1w image data divided by T2w increases the WM to GM tissue contrast. Changes in tissue microstructure (myelin, iron, edema, and brain lesions) affect both T1w and T2w images and have been used separately to study myelination and iron in the human brain (Tyan et al., 2015; Bakshi et al., 2001). Whole brain T1w/T2w ratio maps have provided a sensitive measure, related to myelin and microstructural integrity in multiple sclerosis (Beer et al., 2016) and schizophrenia (Ganzetti et al., 2015). Building on existing findings, we implemented T1w/T2w techniques to map the whole brain volume of ME/CFS patients and healthy controls to potentially reveal important information about the disease pathomechanism.

## 2. Material and methods

### 2.1. Participant recruitment

The study was approved by the local human ethics (HREC/15/QGC/63 and GU:2014/838) committee of the Griffith University and the Gold Coast University Hospital where scanning was performed. Written informed consent was obtained from all individuals. Fifty-six ME/CFS patients and twenty-seven healthy controls (HC) were recruited ranging in age from 24 years to 76 years (see Table 1 for demographic information). Patients and healthy controls were recruited through an online lime survey. Of the fifty-six ME/CFS patients reviewed by a clinician (DS) experienced in ME/CFS, eleven patients with ME/CFS were excluded because they had other core conditions (attention deficit hyperactivity disorder, autoimmune disease, microvascular disease, or body mass index (BMI) > 35). After their exclusion, Forty-five ME/CFS patients met Fukuda (Fukuda, 1994) criteria. Quality of life scores were recorded using the SF-36 questionnaire (Alonso et al., 1995). Healthy controls were included in this study if they had no exclusionary medical disorder and no abnormal physical function.

### 2.2. Clinical measures

Clinical measures incorporated into voxel based T1w/T2w regressions were collected as follows. The 36-item SF36 short form health survey questionnaire (Alonso et al., 1995), was completed by all subjects and the physical and mental summary scores (SF36 physical and SF36 mental) were generated. Heart Rate (HR), Heart Rate Variability (HRV) and Respiration Rate (Resp) were extracted from the power spectra of pulse oximeter and respiration strap data recorded during a

**Table 1**

Demographic characteristics of all participants. M/F = Male/Female, Heart Rate Variability (HRV), SF-36 physical (SF36 phys), Respiration Rate (Resp) and Stroop Effect. SD = standard deviation; n/a = not applicable.

Parameters	ME/CFS mean $\pm$ SD	HC mean $\pm$ SD	P
Age (yrs.)	47.12 $\pm$ 11.67	43.10 $\pm$ 13.7	0.23
M/F	12/33	9/18	n/a
HRV (%)	18.14 $\pm$ 6.63	20.23 $\pm$ 6.69	0.21
SF36 phys	28.32 $\pm$ 14.22	83.22 $\pm$ 18.17	< 0.001
Resp	3.82 $\pm$ 1.14	4.23 $\pm$ 1.36	0.17
Stroop Effect (%)	11.96 $\pm$ 12.09	13.02 $\pm$ 8.89	0.28

15-minute resting state fMRI acquired in the same scanning session (HR and resp from the frequency of the primary peak, and HRV from the width at half maximum of the primary HR peak). Stroop Effect, a cognitive performance measure, was estimated from the Stroop colour-word test conducted during a 15 min task fMRI acquired in the same scanning session (Shan et al., 2018).

### 2.3. MRI scans and data processing

The T1w and T2w data were acquired using a 3 T Skyra MRI scanner (Siemens Healthcare, Erlangen, Germany) with a 64-channel head-neck coil (Nova Medical, Wilmington, USA). Three dimensional T1weighted images were acquired using a T1weighted magnetization prepared rapid gradient-echo (MPRAGE) sequence with repetition time (TR) = 2400 ms, echo time (TE) = 1.81 ms, flip-angle = 8°, acquisition matrix = 224  $\times$  224  $\times$  208, and voxel size 1 mm  $\times$  1 mm  $\times$  1 mm. Three dimensional T2weighted images were acquired using Siemens T2 'SPACE' with TR = 3200 ms, TE = 563 ms, with variable flip angle, matrix size = 256  $\times$  256  $\times$  208, and voxel size 0.88 mm  $\times$  0.88 mm  $\times$  0.9 mm. The total acquisition time for T1w and T2w scans was 8:20 and 5:44 min:sec respectively. MR images were acquired in both patients and healthy controls with the same scanner, using the same scanning parameters.

### 2.4. Image analysis

The T1w and T2w MRI data were pre-processed using a workflow described in (Ganzetti et al., 2015) to generate whole brain T1w/T2w ratio maps. This pre-processing includes co-registration of the T2w image to the T1w image using rigid body transformation (Collignon et al., 1995). Then, bias correction (Ashburner and Friston, 2005; Weiskopf et al., 2011) as implemented in SPM12 was performed separately on T1w and T2w. The input parameters for the bias correction algorithm for smoothing and regularisation were set at their default values. After bias correction, T1w and T2w images were further processed to standardize their intensity using the linear scaling procedure described in (Ganzetti et al., 2014). After normalizing the intensity of T1w and T2w images, their ratio was computed to generate the T1w/T2w map. The processing pipeline for T1w and T2w data is provided as a toolbox 'MRTool' (<https://www.nitrc.org/projects/mrtool/>) incorporated in SPM12 (<https://www.fil.ion.ucl.ac.uk/spm/software/spm12/>). A whole brain T1w/T2w map was computed for each of 45 ME/CFS patients and 27 healthy controls.

### 2.5. ROI based analysis

We evaluated 46 regions of interest (ROIs). Because T1w/T2w responds to myelin and iron concentrations we restricted our analysis here to 40 white matter ROIs and 6 subcortical grey matter ROIs with known elevated iron levels. 38 white matter ROIs were from the ICBM-DTI-81 white-matter label atlas (Mori et al., 2008) and 2 were derived from a voxel-based analysis of T1weighted spin-echo scans in the same subjects as here (Barnden et al., 2018) which detected increased levels (of myelin) in sensorimotor (sensmotor) white matter and decreased levels in the brainstem. The 6 subcortical grey matter ROIs were sourced from the Harvard-Oxford template (Frazier et al., 2005) available with FSL (<https://fsl.fmrib.ox.ac.uk/fsl/fslwiki>) (Smith et al., 2004). The mean T1w/T2w voxel value in each ROI was calculated for each subject. For each ROI, we used a multivariate general linear model to test for significant differences between T1w/T2w values between ME/CFS and HC subjects using age and gender as nuisance covariates with the statistical package for the social sciences (SPSS). The Bonferroni correction was used to adjust for multiple comparisons.

## 2.6. Voxel based statistics

Voxel based statistical comparison of the T1w/T2w maps of the two groups was performed in SPM12. To test for group differences in T1w/T2w a 2-sample T-test was performed controlling for age and gender. Voxel clusters in the T statistic map were defined using an uncorrected voxel p-value threshold  $p < 0.003$  and a cluster size threshold of 150 voxels. Statistical inference was measured with the false discovery rate corrected cluster p value (cluster p-FDR). Significant clusters were overlaid on a T1weighted image (mni\_icbm152\_t1\_tal\_nlin\_sym\_09a). We also performed voxel-based T1w/T2w interaction-with-group regressions with clinical parameters to test for a different relationship in the HC and 43 ME/CFS groups, that is, an abnormal relationship in ME/CFS. The seven clinical parameters used as regressors were HR, HRV, SF-36 phys and mental scores, Resp, Stroop Effect and Stroop Reaction Time. Two ME/CFS subjects with missing clinical parameters were omitted from the group interactions. Two outliers in HRV (one ME/CFS and one HC) and one in Resp (ME/CFS) dominated the interaction results and were omitted.

The FDR after accounting for the multiple interaction regressions performed was also computed. All tests were controlled for age and gender. Cluster locations were identified with the xjview toolbox (<https://www.alivelearn.net/xjview>).

## 3. Results

### 3.1. Region-of-interest analysis

Of the 46 brain ROI evaluated, T1w/T2w was significantly greater ( $p < 0.05$ ) in ME/CFS than in HC in 16 of 40 white matter regions (see Fig. 1) and in all 4 subcortical grey matter regions (see Fig. 2). In no ROI was T1w/T2w lower in ME/CFS than in HC.

Fig. 1 and Table 2 show that in white matter, the lowest T1w/T2w in both groups was in the sensorimotor (sensmotor) ROI, while the highest T1w/T2w was in the inferior longitudinal fasciculus (ILF) ROI. In white matter, the increase in T1w/T2w in ME/CFS relative to HC was most significant in the sensorimotor ( $p = 0.008$ ), right cortico-spinal tract (CST,  $p = 0.009$ ) and right anterior internal capsule (ALIC,  $p = 0.009$ ) ROIs. In subcortical grey matter, right and left putamen (Putam-R/L) and right and left pallidum (Palli-R/L) showed significantly increased T1w/T2w (see Fig. 2). Palli-R and Palli-L showed the highest T1w/T2w values of all white matter and subcortical grey matter regions, and their ME/CFS > HC comparisons were most significant ( $p = 0.003$ ). ME/CFS patients showed higher variability (standard deviation) than healthy controls in 20/24 of the ROIs with significantly increased T1w/T2w in ME/CFS.

### 3.2. T1w/T2w voxel based analysis

#### 3.2.1. Group comparison

Highly significant voxel clusters were detected in the voxel-wise group comparison of T1w/T2w for ME/CFS greater than HC, see Fig. 3 and Table 3. No clusters were detected for ME/CFS < HC. Ascending fibres of the left medial lemniscus (Fig. 3,  $y = -35$ ,  $z = -32$ ) and descending fibres of the right corticospinal tract ( $y = -22$ ,  $z = -32$ ) were enhanced, consistent with enhanced motor support in predominantly right-handed groups. The subcortical putamen, pallidum and thalamus were enhanced, as were the projection tracts of the internal capsule and corona radiata.

#### 3.2.2. Regressions with clinical measures

T1w/T2w Interaction-with-group regressions were performed with 7 clinical scores: SF36 physical, SF36 mental, HR, HRV, Resp, Stroop Effect and mean Reaction Time in Stroop test. Four regressors (Table 4) showed significant clusters with abnormal T1w/T2w regressions in ME/CFS. HRV and Stroop Effect yielded multiple statistically strong clusters

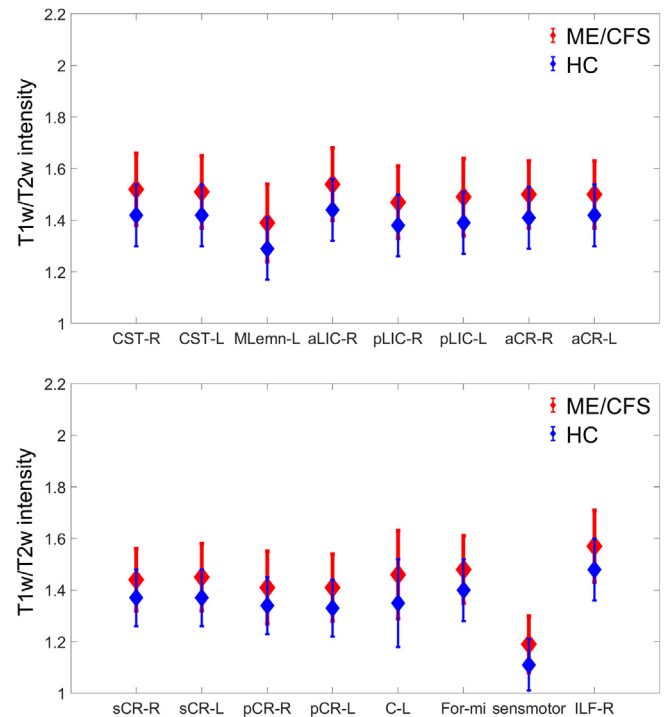


Fig. 1. Mean T1w/T2w in 16 white matter ROIs for ME/CFS (red) and HC (blue). ME/CFS means were significantly greater than HC ( $P < 0.05$ ) in all ROIs. Error bars indicate one standard deviation. CST = cortico-spinal tract, MLeMn = medial lemniscus, aLIC = anterior limb of internal capsule, pLIC = posterior limb of internal capsule, aCR = anterior corona radiata, sCR = superior corona radiata, pCR = posterior corona radiata, C = cingulum, For-mi = forceps minor, sensmotor = sensory motor, ILF = inferior longitudinal fasciculus, (-L = Left, -R = Right). (For interpretation of the references to colour in this figure legend, the reader is referred to the web version of this article.)

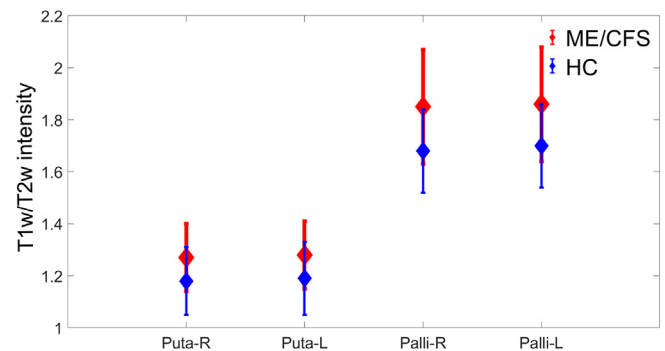


Fig. 2. Mean T1w/T2w in four subcortical grey matter regions for ME/CFS (red) and HC (blue). ME/CFS means were significantly greater than HC ( $P < 0.05$ ) in all ROIs. Error bars indicate one standard deviation. Puta = putamen, Palli = pallidum, (-L = Left, -R = Right). (For interpretation of the references to colour in this figure legend, the reader is referred to the web version of this article.)

despite using a stricter criterion for cluster formation. Fig. 4 shows selected cluster locations for these 4 regressors. The maximum T statistic intensity projections (MIPs from SPM) in Fig. 4A and B emphasise involvement of multiple areas of gyral gray and white matter in the sensorimotor area. Respiration rate showed a significantly different ME/CFS regression in the corpus callosum (Fig. 4C, 5D). In general, significant clusters were quite focal and many were located in gyral WM adjacent to grey matter. When the effects of multiple comparisons from the multiple regressions were evaluated the false discovery rate

**Table 2**  
ROIs with mean T1w/T2w values significantly higher for ME/CFS than for HC, and P-values (after Bonferroni correction). See Figs. 1, 2 captions for ROI abbreviations.

ROI	ME/CFS	HC	Difference	P-value
White Matter regions				
CST-R	1.52 ± 0.14	1.42 ± 0.12	0.1 ± 0.02	0.009
CST-L	1.51 ± 0.14	1.42 ± 0.12	0.9 ± 0.02	0.031
MLemn-L	1.39 ± 0.15	1.29 ± 0.12	0.10 ± 0.03	0.014
aLIC-R	1.54 ± 0.14	1.44 ± 0.12	0.10 ± 0.03	0.009
pLIC-R	1.47 ± 0.14	1.38 ± 0.12	0.09 ± 0.02	0.022
pLIC-L	1.49 ± 0.15	1.39 ± 0.12	0.10 ± 0.03	0.018
aCR-R	1.5 ± 0.13	1.41 ± 0.12	0.09 ± 0.01	0.028
aCR-L	1.5 ± 0.13	1.42 ± 0.12	0.08 ± 0.01	0.027
sCR-R	1.44 ± 0.12	1.37 ± 0.11	0.07 ± 0.01	0.033
sCR-L	1.45 ± 0.13	1.37 ± 0.11	0.08 ± 0.02	0.031
pCR-R	1.41 ± 0.14	1.34 ± 0.11	0.07 ± 0.03	0.041
pCR-L	1.41 ± 0.13	1.33 ± 0.11	0.08 ± 0.04	0.046
C-L	1.46 ± 0.17	1.35 ± 0.17	0.11	0.04
For-mi	1.48 ± 0.13	1.40 ± 0.12	0.08 ± 0.01	0.031
sensorimotor	1.19 ± 0.11	1.11 ± 0.10	0.08 ± 0.01	0.008
ILF-R	1.57 ± 0.14	1.48 ± 0.12	0.09 ± 0.02	0.026
Subcortical Grey matter regions				
Putam-R	1.27 ± 0.13	1.18 ± 0.13	0.09	0.021
Putam-L	1.28 ± 0.13	1.19 ± 0.14	0.09 ± 0.01	0.018
Palli-R	1.85 ± 0.22	1.68 ± 0.16	0.17 ± 0.06	0.004
Palli-L	1.86 ± 0.22	1.7 ± 0.16	0.16 ± 0.06	0.003

remained below 0.05. Fig. 5 illustrates the nature of interaction-with-group regressions with example plots of cluster mean T1w/T2w for 43 ME/CFS and 27 HC in four clusters from four regressors. Variance associated with age and gender was removed from the plotted means.

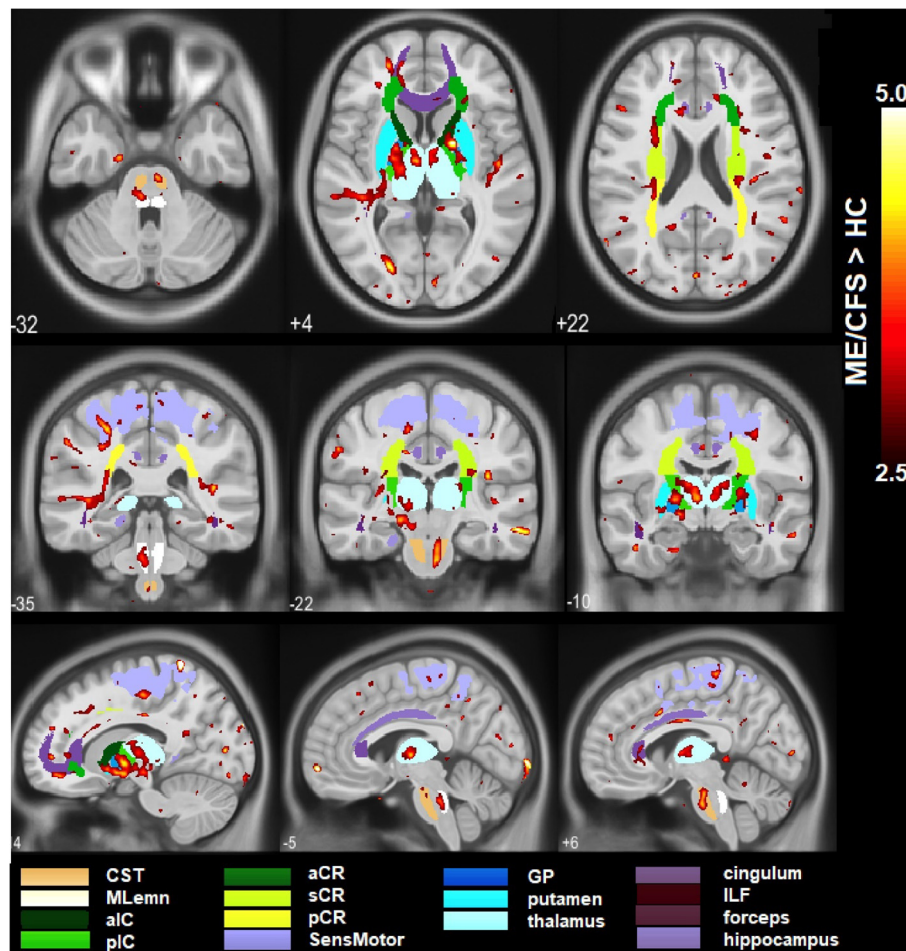


**Fig. 3.** T1w/T2w results for ME/CFS > HC for both voxel- and ROI-based analysis. Voxels from the SPM group comparison (red-yellow) have  $T > 2.5$ . Multiple large clusters were significant. The atlas ROIs where significant increases in ME/CFS were detected are shown as uniformly coloured areas according to legend. SPM and ROI increases in T1w/T2w occurred in white matter (WM) of the cortico-spinal tract (CST), medial lemniscus (MLemn), corpus callosum, and projection tracts of the posterior internal capsule (pIC), corona radiata (anterior, superior and posterior – aCR, sCR, pCR) and gyral sensorimotor (SensMotor) WM; as well as in the subcortical grey matter of the putamen, pallidum (GP), and thalamus. (For interpretation of the references to colour in this figure legend, the reader is referred to the web version of this article.)

Except for (Fig. 5B), the group means of the clinical scores were not significantly different between HC and ME/CFS.

#### 4. Discussion

We used the T1w/T2w ratio to study tissue microstructural changes in ME/CFS patients and healthy controls. The most striking finding was that T1w/T2w values were significantly higher in ME/CFS than in HC, both in white matter and subcortical grey matter structures, indicating higher levels of myelin and/or iron. This study is the first to report findings for increased T1w/T2w in ME/CFS patients.

We performed both ROI- and voxel-based analysis. Here, we selected ROIs in white matter and subcortical grey matter.

The ROI-based analysis showed significantly elevated T1w/T2w in ME/CFS in 16 of 40 white matter regions and in four subcortical grey matter regions (see Fig. 2). This was despite applying the strict Bonferroni correction for multiple comparisons. Elevated WM T1w/T2w occurred in descending and ascending cortico-spinal white matter tract ROIs in the brainstem (one-sided), and projection (internal capsule and corona radiata) tracts, but in only one association tract (ILF) (see Fig. 1),

Voxel-based analysis detected clusters with increased T1w/T2w in ME/CFS with remarkably strong statistical inference particularly in the subcortical grey matter structures of the putamen, globus pallidus and thalamus (see Fig. 3). It also confirmed increased T1w/T2w in one-sided brainstem corticospinal tracts. Voxel-based analysis did not detect as many WM differences as the ROI-based approach due to the higher sensitivity of the latter.

Stuber et al. (Stüber et al., 2014) demonstrated that in WM, 90% of  $R1 (= 1/T1)$  contrast derives specifically from myelin, whereas in GM,

**Table 3**

Cluster statistics of T1w/T2w group comparison for ME/CFS greater than HC. The voxel P threshold for cluster formation of 0.003 was relaxed to 0.005 for the brainstem clusters. Voxel volume = 0.001 ml.

Area	Peak X Y Z mm	cluster size (voxels)	voxel P threshold	cluster p-FDR
Global pallidus	-14 -5 -4	395	0.003	9e <sup>-5</sup>
Paracentral_Lobule	9 -33 63	258	0.003	0.002
Posterior Corona Radiata	-26 -28 11	267	0.00	0.002
Precuneus_Left	-14 -49 74	227	0.003	0.003
putamen	19 0 6	182	0.003	0.01
Cerebro-spinal Tract	4 -20 -32	279	0.005	0.002
Medial Lemniscus	-10 -31 -39	259	0.005	0.003

81% of R2\* (=1/T2\*) contrast derives specifically from iron. T1 increases with increasing myelin while T2 decreases with increasing iron. Thus, both increasing myelin and increasing iron will increase T1w/T2w. It is known that the subcortical GM of the pallidum, putamen and thalamus have relatively high iron levels (Bakshi et al., 2001). Here, the pallidum ROIs showed the highest T1w/T2w levels in both HC and ME/CFS (Fig. 2, Table 1). The pallidum also showed the highest relative increase in ME/CFS. Although their relative contributions to T1 and T2\* contrast suggest T1w/T2w is more strongly influenced by iron in GM and by myelin in WM (Stüber et al., 2014). However, in WM of the internal capsule and anterior corona radiata, a myelin rather than iron increase in ME/CFS was supported by correlations with ME/CFS severity for T1wSE but not T2wSE (Barnden et al., 2015).

T1w/T2w has been used to map whole brain myelination in healthy controls (Ganzetti et al., 2014) and to study myelin abnormalities in multiple sclerosis and schizophrenia (Beer et al., 2016; Ganzetti et al., 2015) which exhibited decreases in T1w/T2w. A recent ME/CFS study, Barnden et al. (2018) showed that higher T1wSE values in sensorimotor (sensmotor) white matter were reciprocally related to T1wSE decreases in the brainstem. It was suggested that increased myelin in sensmotor WM was a thalamus-mediated compensatory response to compromised ascending signals from the brainstem. It is possible that T1w/T2w detects this increase across wider areas of the brain. Increased T1w/T2w here in the (descending) cortico-spinal tract and (ascending) medial

lemniscus indicates fundamental changes to brain-body communication in ME/CFS. Indeed, most of the structures with increased T1w/T2w were involved with sensorimotor function. A diffusion study has reported higher values of fractional anisotropy (FA) in the right arcuate fasciculus in ME/CFS due to increase in myelination (Tyan et al., 2015; Sakuma et al., 1991) which is adjacent to the right ILF region reported here.

High T1w/T2w in the thalamus, putamen, and pallidum is expected due to their high iron levels (Bakshi et al., 2001; Drayer et al., 1987), and the ME/CFS increases here may indicate abnormal deposition of iron during ME/CFS disease progression. Iron mediated hyperintensity in T1 weighted images was reported in the globus pallidus gray matter to reach intensity levels close to white matter (Vymazal et al., 1995). In multiple sclerosis patients, reduced T2 weighted signal intensity was reported (Bakshi et al., 2001) (Drayer et al., 1987) in the thalamus, putamen, and globus pallidus that was suggested to derive from increased iron deposition. Higher values of myelination and iron in ME/CFS patients can derive from perturbed cell membrane calcium (Ca<sup>2+</sup>) transport (Núñez and Hidalgo, 2019), which has been reported in ME/CFS patients (Cabanas et al., 2019). Ca<sup>2+</sup> ion channels at TRPM3 receptors are widely distributed in brain white matter, cortex, thalamus and hippocampus rendering the brain sensitive to their dysfunction (Hong et al., 2020). The low T1w/T2w intensity values in the sensorimotor and MLEmn-L white matter regions could relate to the reduced

**Table 4**

Significant clusters from T1w/T2w voxel-wise interaction-with-group regressions with five clinical regressors. Clusters were formed with an uncorrected voxel P threshold of 0.003 (or 0.001 for Stroop Effect) and exceeded 150 voxels in extent. The cluster P is FDR-corrected for multiple comparisons. The sign of the regressor is the sign of the slope of the regression for the ME/CFS group. BA = Brodmann Area, L = left and R = right. \* indicates white matter clusters (adjacent to the grey matter area reported). Two outliers were omitted from the HRV and one from the Resp analysis.

Regressor	Area (gyrus)	Fig.	Peak X Y Z mm	cluster size (voxels)	cluster P
- HRV	cingulate cortex	4A, 5A	-2 11 26	306	0.001
	precentral		-8 -18 79	235	0.003
	BA6		33 7 64	224	0.003
	BA-6		42 -7 56	187	0.007
	BA-7		26 -68 57	169	0.009
	BA6		-4 -10 72	174	0.009
- SF36 phys	*L middle temporal	4D, 5B	-44 -43 2	337	0.002
	*R middle temporal	4D	48 -38 -5	301	0.007
	BA7		-17 -55 66	252	0.007
	*L cuneus		-25 -86 29	190	0.014
	*BA40		-41 -33 34	186	0.017
	BA8		22 15 49	160	0.024
+ Resp	corpus callosum	4C, 5D	13 2 29	579	3e <sup>-7</sup>
	Cerebral WM		26 -47 21	316	2e <sup>-4</sup>
	Middle Temporal Gyrus		48 -26 -8	162	0.02
	Cerebellum_Crus2_R		-50 -46 -40	160	0.02
+ Stroop Effect	*BA3	5C	51 -17 55	266	7e <sup>-5</sup>
	*BA2	4B	56 -27 36	207	3e <sup>-4</sup>
	*R middle temporal		33 -68 17	208	3e <sup>-4</sup>
	*L postcentral	4B	-36 -26 39	178	0.001
	*middle temporal		-40 -60 1	162	0.001

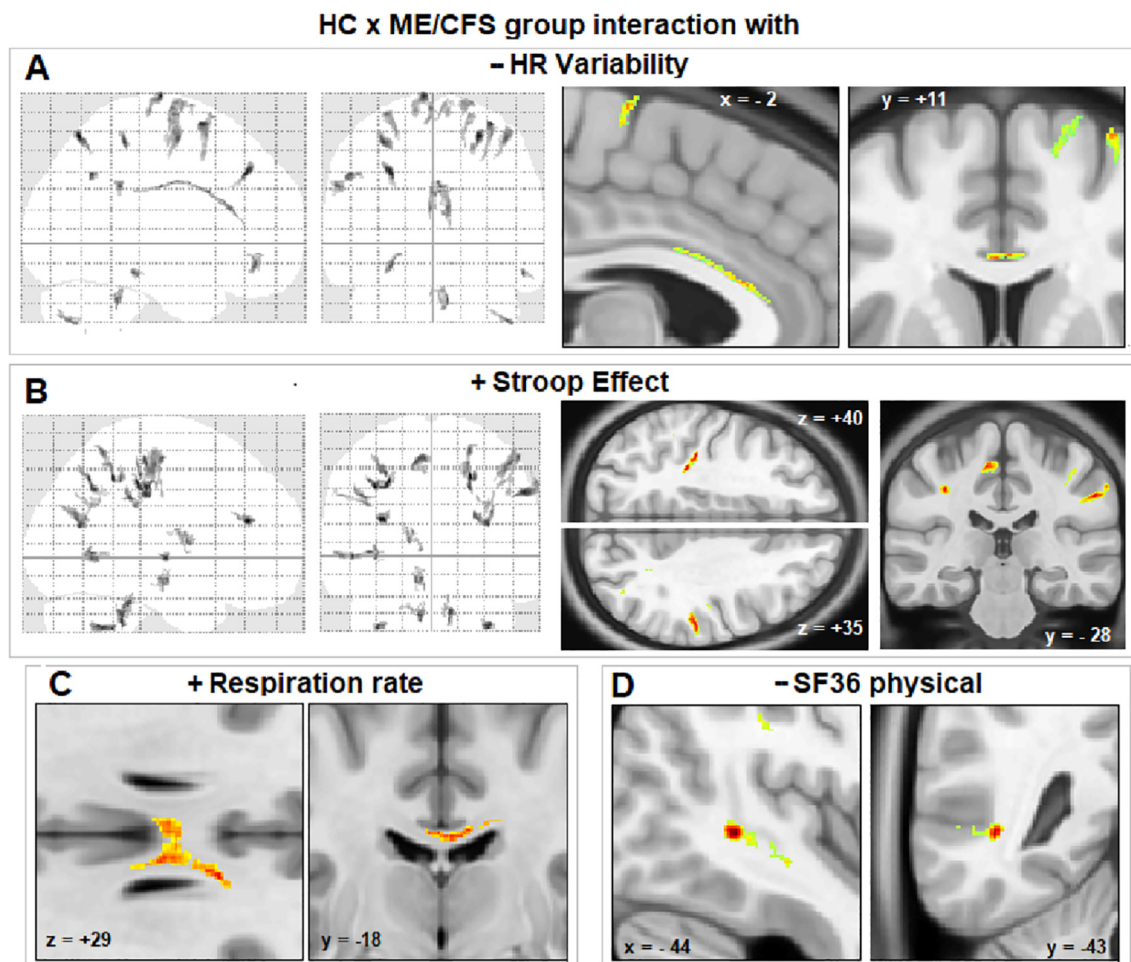


**Fig. 4.** Examples of significant clusters from T1w/T2w voxel-based interaction-with-group regressions for 4 clinical regressors. Voxels shown in colour have  $P$  (uncorrected)  $< 0.003$ . The two left hand panels in A and B show voxel T statistic maximum projections (MIPs) for voxels with different ME/CFS and HC regressions and highlight their sensorimotor gyral distribution and, in A, the elongated cingulate cortex cluster. The right-hand panels of A and B and C, and D show the colour-encoded T statistic in sections through individual clusters superimposed on a reference brain. Except for A, the clusters are located in white matter.

iron levels outside of subcortical regions (Choi et al., 2015), or the sulci included in the large sensorimotor region.

#### 4.1. Interaction-with-group regressions

Voxel-based T1w/T2w interaction-with-group regressions with clinical measures yielded multiple clusters with strong statistical inference (Table 3, Figs. 4, 5). The HRV cingulate cortex cluster is consistent with findings that the midcingulate cortices are involved with parasympathetic control (Beissner et al., 2013). As in previous analyses, we suggest that in HC normal variability in local myelin or iron leads to the observed variation in (regression with) clinical measures. In ME/CFS however, we suggest that the extended (and variable) increases in myelin and/or iron disrupt some connectivity patterns and affect clinical measures in such a way that their normal association with local levels is inverted. Indeed, in the same subjects as were studied here, fMRI studies demonstrated that variations in the SF36 physical score could be partly explained by variation in default mode network connectivity and the complexity of BOLD time series (Shan et al., 2018).

Changed T1w/T2w in ME/CFS in both white matter and subcortical grey matter structures does not resolve whether myelin or iron or both are involved in the pathological changes. To address this limitation, it is necessary to develop new imaging methods to separate myelin and iron. Longitudinal studies may better reveal how T1w/T2w signal intensity changes over time in different structures in ME/CFS patients.

## 5. Conclusion

We implemented T1w/T2w techniques to map differences in brain structure between ME/CFS and healthy controls. Using both region- and voxel-based analysis, we found T1w/T2w values were significantly higher in ME/CFS in white matter tracts involved in sensorimotor communication, sensorimotor gyral white matter, and subcortical grey matter structures involved with motor control. This is opposite to the decreases reported in other neurological disorders. The highest T1w/T2w signal intensity values were reported in the pallidum with its high iron content. Overall, our findings suggest that T1w/T2w is highly sensitive to different brain structure in ME/CFS patients relative to healthy controls.

#### CRedit authorship contribution statement

**Kiran Thapaliya:** Methodology, Writing - original draft, Writing - review & editing. **Sonya Marshall-Gradisnik:** Supervision, Writing - review & editing. **Don Staines:** Supervision, Writing - review & editing. **Leighton Barnden:** Supervision, Methodology, Writing - review & editing.

#### Acknowledgement

This research was supported by the Stafford Fox Medical Research Foundation, the Mason Foundation, Mr. Douglas Stutt, Blake Beckett

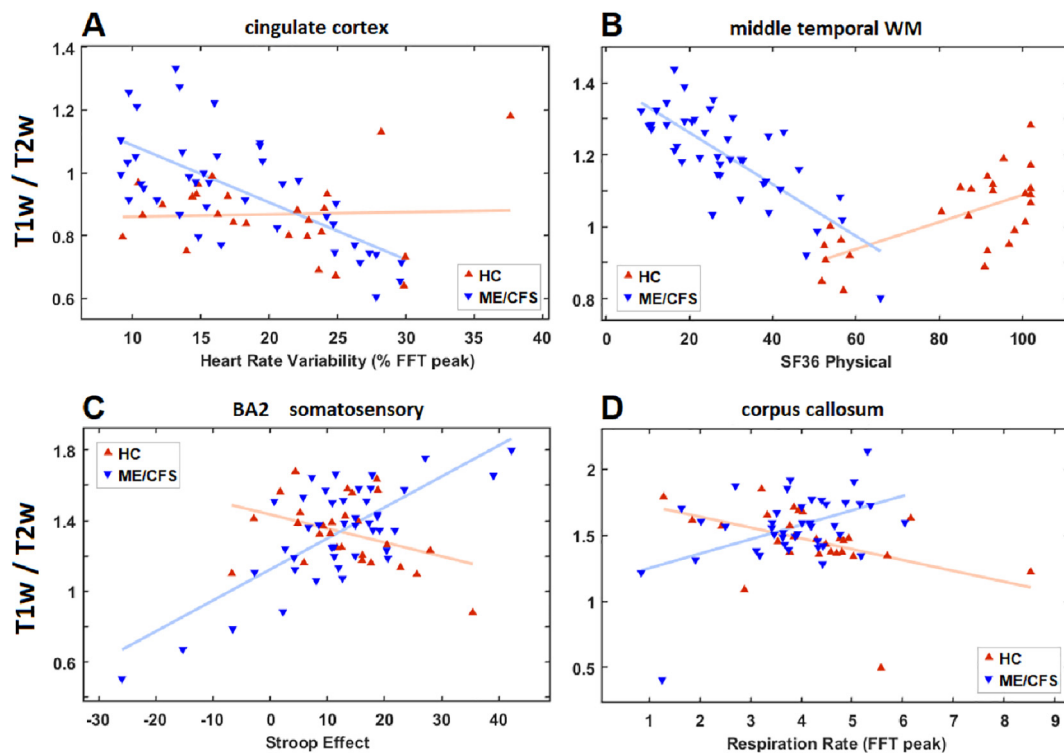


**Fig. 5.** Plots for 27HC and 43 ME/CFS subjects of T1w/T2w cluster means versus four clinical measures (see X axis label). A. Heart Rate Variability (cluster  $P = 0.001$  in cingulate cortex – see Fig. 4A); B. SF36 physical score (cluster  $p = 0.0005$  in middle temporal lobe – see Fig. 4D); C. Stroop Effect ( $p = 0.003$  in Brodmann area (BA) 2 – see Fig. 4B  $z = +35$ ); D. Respiration Rate (cluster  $p = 3e^{-7}$  in the corpus callosum – see Fig. 4C). Means were computed after removing age and gender variance.

Foundation, Alison Hunter Memorial Foundation, the McCusker Charitable Foundation, Buxton Foundation, Mr and Mrs Stewart, Henty Community, Henty Lions Club and the Change for ME Charity. We acknowledge the valuable support of Zack Shan, Kevin Finegan and Sandeep Bhuta.

## References

- Fukuda, K., 1994. The chronic fatigue syndrome: a comprehensive approach to its definition and study. *Ann. Intern. Med.* 121 (12), 953.
- Cockshell, S.J., Mathias, J.L., 2010. Cognitive functioning in chronic fatigue syndrome: a meta-analysis. *Psychol. Med.* 40 (8), 1253–1267.
- Faro, M., Sàez-Francàs, N., Castro-Marrero, J., Aliste, L., Fernández de Sevilla, T., Alegre, J., 2016. Gender differences in chronic Fatigue Syndrome. *Reumatol. Clín. Engl. Ed.* 12 (2), 72–77.
- Schwartz, R.B., Garada, B.M., Komaroff, A.L., et al., 1994. Detection of intracranial abnormalities in patients with chronic fatigue syndrome: comparison of MR imaging and SPECT. *AJR Am. J. Roentgenol.* 162 (4), 935–941.
- Zeineh, M.M., Kang, J., Atlas, S.W., et al., 2014. Right arcuate fasciculus abnormality in chronic Fatigue Syndrome. *Radiology.* 274 (2), 517–526.
- Finkelmeyer, A., He, J., Maclachlan, L., et al., 2018. Grey and white matter differences in Chronic Fatigue Syndrome – A voxel-based morphometry study. *NeuroImage Clin.* 17, 24–30.
- de Lange, F.P., Kalkman, J.S., Bleijenberg, G., Hagoort, P., van der Meer, J.W.M., Toni, I., 2005. Gray matter volume reduction in the chronic fatigue syndrome. *NeuroImage* 26 (3), 777–781.
- Barnden, L.R., Shan, Z.Y., Staines, D.R., et al., 2018. Hyperintense sensorimotor T1 spin echo MRI is associated with brainstem abnormality in chronic fatigue syndrome. *NeuroImage Clin.* 20, 102–109.
- Puri, B.K., Jakeman, P.M., Agour, M., et al., 2012. Regional grey and white matter volumetric changes in myalgic encephalomyelitis (chronic fatigue syndrome): a voxel-based morphometry 3 T MRI study. *Br. J. Radiol.* 85 (1015), e270–e273.
- Buchwald, D., Cheney, P.R., Peterson, D.L., et al., 1992. A chronic illness characterized by fatigue, neurologic and immunologic disorders, and active human herpesvirus type 6 infection. *Ann. Intern. Med.* 116 (2), 103–113.
- Okada, T., Tanaka, M., Kuratsune, H., Watanabe, Y., Sadato, N., 2004. Mechanisms underlying fatigue: a voxel-based morphometric study of chronic fatigue syndrome. *BMC Neurol.* 4 (1), 14.
- Barnden, L.R., Crouch, B., Kwiatek, R., Burnet, R., Del Fante, P., 2015. Evidence in chronic fatigue syndrome for severity-dependent upregulation of prefrontal myelination that is independent of anxiety and depression. *NMR Biomed.* 28 (3), 404–413.

- Barnden, L.R., Shan, Z.Y., Staines, D.R., et al., 2019. Intra brainstem connectivity is impaired in chronic fatigue syndrome. *NeuroImage Clin.* 24, 102045.
- Boissoneault, J., Letzen, J., Lai, S., et al., 2016. Abnormal resting state functional connectivity in patients with chronic fatigue syndrome: an arterial spin-labeling fMRI study. *Magn. Reson. Imaging.* 34 (4), 603–608.
- Natelson, B.H., Cohen, J.M., Brassloff, I., Lee, H.J., 1993. A controlled study of brain magnetic resonance imaging in patients with the chronic fatigue syndrome. *J. Neurol. Sci.* 120 (2), 213–217.
- Cope, H., David, A.S., 1996. Neuroimaging in chronic fatigue syndrome. *J. Neurol. Neurosurg. Psychiatry* 60 (5), 471–473.
- Ganzetti, M., Wenderoth, N., Mantini, D., 2016. Whole brain myelin mapping using T1- and T2-weighted MR imaging data. *Front. Hum. Neurosci.* 2014;8. <http://www.ncbi.nlm.nih.gov/pmc/articles/PMC4151508/>. Accessed August 11, 2016.
- Uddin, M.N., Figley, T.D., Figley, C.R., 2018. Effect of echo time and T2-weighting on GRASE-based T1w/T2w ratio measurements at 3T. *Magn. Reson. Imaging.* 51, 35–43.
- Tyan, A.E., McKinney, A.M., Hanson, T.J., Truwit, C.L., 2015. Comparison of spin-echo and gradient-echo T1-weighted and spin-echo T2-weighted images at 3T in evaluating term-neonatal myelination. *Am. J. Neuroradiol.* 36 (2), 411–416.
- Bakshi, R., Dmochowski, J., Shaikh, Z.A., Jacobs, L., 2001. Gray matter T2 hypointensity is related to plaques and atrophy in the brains of multiple sclerosis patients. *J. Neurol. Sci.* 185 (1), 19–26.
- Beer, A., Biberacher, V., Schmidt, P., et al., 2016. Tissue damage within normal appearing white matter in early multiple sclerosis: assessment by the ratio of T1- and T2-weighted MR image intensity. *J. Neurol.* 263 (8), 1495–1502.
- Ganzetti, M., Wenderoth, N., Mantini, D., 2015. Mapping pathological changes in brain structure by combining T1- and T2-weighted MR imaging data. *Neuroradiology* 57 (9), 917–928.
- Alonso, J., Prieto, L., Anto, J.M., 1995. The Spanish version of the SF-36 Health Survey (the SF-36 health questionnaire): an instrument for measuring clinical results. *Med. Clín.* 104 (20), 771–776.
- Shan, Z.Y., Finegan, K., Bhuta, S., et al., 2018. Decreased connectivity and increased blood oxygenation level dependent complexity in the default mode network in individuals with Chronic Fatigue Syndrome. *Brain Connect.* 8 (1), 33–39.
- Collignon, A., Maes, F., Delaere, D., Vandermeulen, D., Suetens, P., Marchal, G., 1995. Automated multi-modality image registration based on information theory. *Inf. Process. Med. Imaging* 263–274.
- Ashburner, J., Friston, K.J., 2005. Unified segmentation. *Neuroimage* 26 (3), 839–851.
- Weiskopf, N., Lutti, A., Helms, G., Novak, M., Ashburner, J., Hutton, C., 2011. Unified segmentation based correction of R1 brain maps for RF transmit field inhomogeneities (UNICORT). *Neuroimage* 54 (3), 2116–2124.
- Mori, S., Oishi, K., Jiang, H., et al., 2008. Stereotaxic white matter atlas based on diffusion tensor imaging in an ICBM template. *NeuroImage.* 40 (2), 570–582.
- Frazier, J.A., Chiu, S., Breeze, J.L., et al., 2005. Structural Brain Magnetic Resonance Imaging of Limbic and Thalamic Volumes in Pediatric Bipolar Disorder. *Am J*

- Psychiatry. 162 (7), 1256–1265.
- Smith, S.M., Jenkinson, M., Woolrich, M.W., et al., 2004. Advances in functional and structural MR image analysis and implementation as FSL. *NeuroImage*. 23, S208–S219.
- Stüber, C., Morawski, M., Schäfer, A., et al., 2014. Myelin and iron concentration in the human brain: A quantitative study of MRI contrast. *NeuroImage*. 93, 95–106.
- Sakuma, H., Nomura, Y., Takeda, K., et al., 1991. Adult and neonatal human brain: diffusional anisotropy and myelination with diffusion-weighted MR imaging. *Radiology* 180 (1), 229–233.
- Drayer, B., Burger, P., Hurwitz, B., Dawson, D., Cain, J., 1987. Reduced signal intensity on MR images of thalamus and putamen in multiple sclerosis: increased iron content? *Am. J. Roentgenol.* 149 (2), 357–363.
- Vymazal, J., Brooks, R.A., Patronas, N., Hajek, M., Bulte, J.W.M., Di Chiro, G., 1995. Magnetic resonance imaging of brain iron in health and disease. *J. Neurol. Sci.* 134, 19–26.
- Núñez, M.T., Hidalgo, C., 2019. Noxious iron–calcium connections in neurodegeneration. *Front. Neurosci.* 2019;13. <https://www.frontiersin.org/articles/10.3389/fnins.2019.00048/full>. Accessed July 24, 2020.
- Cabanas, H., Muraki, K., Balinas, C., Eaton-Fitch, N., Staines, D., Marshall-Gradisnik, S., 2019. Validation of impaired Transient Receptor Potential Melastatin 3 ion channel activity in natural killer cells from Chronic Fatigue Syndrome/Myalgic Encephalomyelitis patients. *Mol. Med.* 25 (1), 14.
- Hong, C., Jeong, B., Park, H.J., et al., 2020. TRP channels as emerging therapeutic targets for neurodegenerative diseases. *Front. Physiol.* 11. <https://www.frontiersin.org/articles/10.3389/fphys.2020.00238/full>. Accessed July 24, 2020.
- Choi, J., Dickson, P., Calabrese, E., et al., 2015. Predicting degree of myelination based on diffusion tensor imaging of canines with mucopolysaccharidosis type I. *Neuroradiol. J.* 28 (6), 562–573.
- Beissner, F., Meissner, K., Bär, K.-J., Napadow, V., 2013. The autonomic brain: an activation likelihood estimation meta-analysis for central processing of autonomic function. *J. Neurosci.* 33 (25), 10503–10511.
- Shan, Z.Y., Finegan, K., Bhuta, S., et al., 2018. Brain function characteristics of chronic fatigue syndrome: a task fMRI study. *NeuroImage Clin.* 19, 279–286.